

Special edition

A numerical investigation on the wind-induced response of a high-rise building considering the soil-structure interaction

Uma investigação numérica sobre a resposta induzida pelo vento de um edifício alto considerando a interação solo-estrutura

Michael Renê Mix Visintainer¹ , Alexandre Luis Braun¹ 

¹ Universidade Federal do Rio Grande do Sul, Porto Alegre, RS, Brazil

ABSTRACT

In the present work, a numerical investigation is carried out to evaluate the wind-induced response of a standard tall building model resting on a deformable soil. The numerical model is developed in this work from a partitioned coupling scheme, in which the physical media involved are solved sequentially, and may present independent discretization and solution methods. The problem is spatially discretized using eight-node hexahedral isoparametric elements with underintegration techniques. The fundamental flow equations are kinematically described using an Arbitrary Lagrangian-Eulerian (ALE) formulation, and numerically solved using the explicit two-step Taylor-Galerkin scheme. Structure and soil are considered as deformable elastoplastic media, using a corotational approach to deal with physical and geometric nonlinearities. A three-dimensional contact formulation based on the penalty method is used to perform the load transfer between soil and foundation. A hybrid parallelization model based on CUDA-OpenMP techniques is employed to improve the processing performance. Numerical results obtained from aeroelastic analyses are compared with numerical and wind tunnel measurements reported by other authors. The results demonstrated that the soil-structure interaction affected the building's response to the wind action and that the aeroelastic instability due to vortex shedding can be considerably reduced with the soil presence

Keywords: Computational wind engineering; Fluid-structure-soil interaction; Finite element method; Contact mechanics

RESUMO

No presente trabalho, uma investigação numérica é realizada para avaliar a resposta induzida pelo vento de um modelo de edifício padrão alto apoiado em um solo deformável. O modelo numérico é

desenvolvido neste trabalho a partir de um esquema de acoplamento particionado, no qual os meios físicos envolvidos são resolvidos de forma sequencial, podendo apresentar métodos de discretização e solução independentes. O problema é discretizado espacialmente usando elementos hexaédricos isoparamétricos de oito nós com técnicas de integração reduzida. As equações fundamentais do escoamento são descritas cinematicamente através de uma formulação arbitrária lagrangiana-euleriana (ALE) e resolvidas numericamente usando o esquema explícito de dois passos de Taylor-Galerkin. A estrutura e o solo são considerados como meios deformáveis elastoplásticos, sendo empregada uma abordagem corrotacional para lidar com as não linearidades física e geométrica. Um algoritmo de contato tridimensional baseado no método da penalidade é utilizado para realizar a transferência de esforços entre o solo e a fundação. Um modelo híbrido de paralelização baseado nas técnicas CUDA-OpenMP é empregado para melhorar o desempenho de processamento. Resultados numéricos obtidos das análises aeroelásticas são comparados com resultados numéricos e de túnel de vento relatados por outros autores. Os resultados demonstraram que a interação solo-estrutura afetou a resposta do edifício à ação do vento e que a instabilidade aeroelástica devido ao desprendimento de vórtices pode ser consideravelmente reduzida com a presença do solo.

Palavras-chave: Engenharia do vento computacional; Interação fluido-estrutura-solo; Método dos elementos finitos; Mecânica do contato

1 INTRODUCTION

The design of slender high-rise and light weight structures has increased in the last decades due to the developments in material technology and construction techniques. As a result, new tall structures are more sensitive to the wind loads and the wind-induced vibration can lead to aeroelastic instability phenomenon. In this sense, experimental analysis in wind tunnels consists in the most important tool to evaluate the wind effects on structures.

It is observed that, in general, the tests in wind tunnels are carried out considering ideal support conditions, in other words, ignoring the effects of soil-foundation-structure when considering the foundation resting on a rigid base or simulating only the physical properties of the structure in the case of aeroelastic analysis (Melbourne, 1980; Thepmongkorn *et al.*, 1999). However, it is known that the soil presence in the numerical model leads to damping increase and lower structural stiffness (Jia, 2018), modifying the dynamic structural response (Menglin *et al.*, 2011). Therefore, it is clear that the overall response of the structure is directly affected by the interaction between structure, foundation and soil.

On the other hand, numerical simulations have become a very attractive tool for Wind Engineering studies due to the increasing advance in computer technology, which can provide data that is often difficult to obtain in wind tunnel tests (Blocken, 2014). However, fluid-structure numerical models developed for Computational Wind Engineering (CWE) applications also usually neglect the interaction effects of superstructure with foundation and soil (Braun and Awruch, 2009; Huang *et al.*, 2007).

An important aspect to consider in wind tunnels consists in the additional challenge to simulate the correct behavior of the soil in small-scale models, mainly due to the similarity conditions to be respected and, especially, for soils where the confining pressure is an important feature to be simulated. In this case, a numerical model may be the best alternative to resolve this problem.

Studies dedicated to the soil-structure interaction applied to tall buildings under wind load are scarce and the soil-structure interaction is usually restricted to earthquake problems (Liu *et al.*, 2008; Venanzi *et al.*, 2014). The effects of soil-structure interaction on structural response to wind action was investigated by Novak and Hifnawy (1988) considering an analytical approach. This study pointed out that the structural response to vortex shedding can be substantially reduced depending on the foundation stiffness.

In recent work, Shirkhanghah and Kalehsar (2022) used the software Abaqus to perform aerodynamic and aeroelastic analyses of the CAARC (Commonwealth Advisory Aeronautical Council) standard tall building. It was possible to verify that the soil presence had a strong influence on the building displacements, but the aeroelastic instability induced by vortex shedding phenomenon was not investigated. A similar formulation was also employed by Shirkhanghah and Kalehsar (2020) to evaluate the effects of cross-section and slenderness on the dynamic response of the CAARC building resting on a deformable soil.

It is also possible to observe that the numerical simulation of fluid-structure-soil interaction consists in a problem of high computational demand, requiring some

parallelization technique. One of the ways to speed up the solution of CWE problems is the use of OpenMP (Open Multi-Processing) parallelization technique (Madalozzo *et al.*, 2014). Despite the performance improvement when compared to the corresponding serial algorithm, models using OpenMP may still require weeks, or even months, of computational processing time. In contrast, Graphics Processing Units (GPUs) have been acquiring significant improvements in memory and processing capacity with each new generation, demonstrating an attractive alternative for high-performance applications especially after the development of the CUDA (Compute Unified Device Architecture) approach (Thibault and senocak, 2012).

Therefore, the main objective of the present work is to evaluate the wind-induced response of the CAARC standard tall building model resting on a deformable soil. An important topic in this paper consists in the attempt to investigate the aeroelastic instability induced by vortex shedding phenomenon, known as *lock-in*. In addition, the performance of the developed CUDA-OpenMP model is compared with the corresponding serial algorithm and different parallelization approaches. Numerical results obtained from aeroelastic analyses are compared with numerical and wind tunnel measurements reported by other authors.

2 NUMERICAL MODEL

The air is modeled in the present work as a three-dimensional incompressible turbulent flow and remains in constant temperature. In this case, the fundamental equations involving viscous fluids are defined by the well-known Navier-Stokes equations and the mass conservation equation. Taking into account that the immersed structure may show displacements, vibrations and deformations during the fluid-structure interaction process, an Arbitrary Lagrangian-Eulerian (ALE) description is introduced in the fundamental equations. The present numerical model for the wind flow analysis is performed using the explicit two-step Taylor-Galerkin, where eight-node hexahedral elements with one-point quadrature are used for spatial discretization.

Turbulent flows are very common in problems of fluid dynamics, although they are very difficult to simulate numerically due to the smaller scales observed in the turbulence flow, which are associated with the smaller eddies of the flow field. Considering the FEM context, in theory, any problem could be solved using the fundamental equations but the element dimension is directly related to the smaller scales, leading to a high computational cost. Therefore, a turbulence model is needed to reproduce turbulence effects more efficiently.

In the present work, the analysis of turbulent flows is performed considering the Large Eddy Simulation (LES) with dynamic sub-grid scale model. In the same manner, the fundamental equations for structural dynamics under isothermal condition are defined by momentum and mass conservation equations, in addition to a material constitutive law. The numerical model for elastic body (structure and soil subsystems) analysis is obtained applying the Bubnov-Galerkin's weighted residual scheme on the fundamental equation, considering a FEM framework, which leads to the well-known dynamic equilibrium equation. The element matrices and variables are evaluated using the eight-node hexahedral finite element formulation considering two underintegration techniques (one-point quadrature and B method). These two underintegration techniques are also utilized to suppress volumetric and locking effects from the finite element formulation.

Structure and soil are considered taking into account an elastoplastic material model, where a corotational approach is adopted to deal with physical and geometric nonlinearities. Note that the contact formulation is also inherently nonlinear, since the contact surface is not known previously. In order to maintain objectivity of the stress updates in the corotational system, stress rate measures are performed in this work using the Truesdell rate tensor.

The system of nonlinear equations obtained in the structural analysis is solved using the Newton-Raphson method, considering an incremental-iterative approach. In addition, the equation of motion is discretized in the time domain employing the Generalized- α method.

Load transfer between soil and structure is performed in this work using a three-dimensional contact model based on the penalty method with a node-to-surface formulation, where a five-node contact element is defined by the four target nodes (hexahedral element face) and the slave node. On the other hand, a partitioned coupling scheme is employed for fluid-structure analysis, where subcycling and synchronizing algorithms for non-matching meshes between the fluid and structure fields are also included in the present model.

An important aspect of FEM models is the difficulty of simulating semi-infinite medium problems, especially for dynamic problems, since the energy can be trapped inside the mesh due to reflection of waves when a fixed boundary condition is utilized. Therefore, infinite elements are used in this work at the boundary of soil-structure problems to provide a quiet boundary, where no wave reflections are expected. The infinite element is responsible for providing stiffness in static analysis and for providing damping, through standard viscous boundaries, in dynamic analysis.

Finally, due to the high computational demand, a hybrid CUDA-OpenMP approach is employed in this work to improve processing efficiency for large scale simulations, where the structural analysis is performed by the CPU (Central Processing Units) and wind flow analysis is performed by the GPU (Graphics Processing Units). A detailed description about the present numerical model may be found in Visintainer (2022).

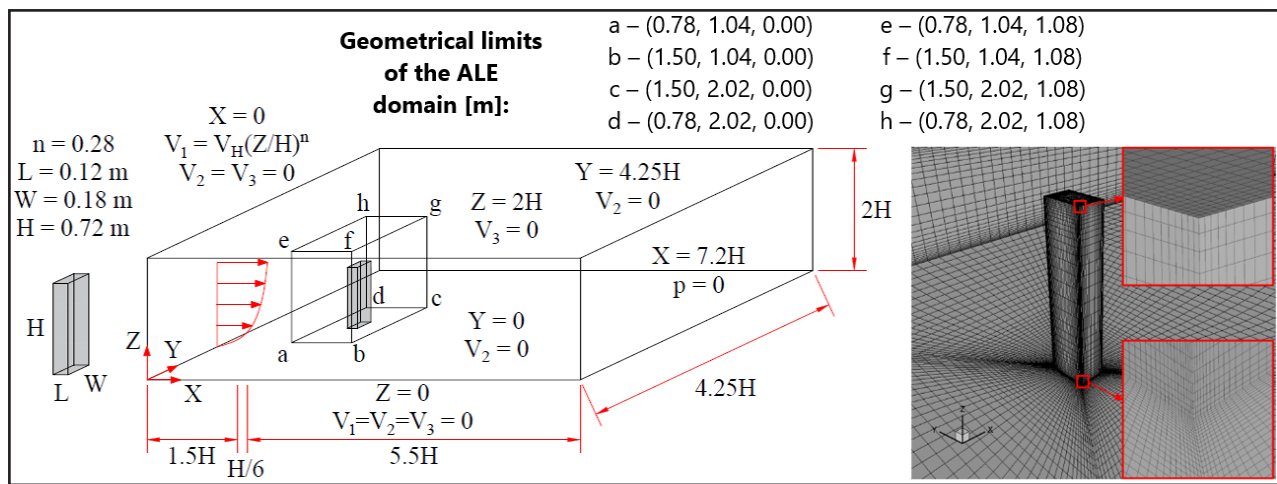
3 NUMERICAL RESULTS

The CAARC standard tall building, characterized as a rectangular prism with flat walls and with no architectural element, is studied in the present example. The building full-scale dimensions are defined as follows: height (H) = 180 m, length (L) = 30 m and width (W) = 45 m. The CAARC building was extensively analyzed in different wind tunnels as a standard model to investigate the wind effects on tall buildings. Geometrical characteristics of the computational domain and boundary conditions adopted in the present simulations are shown in Figure 1, where the mesh configuration employed

for the fluid domain is also presented.

A geometric scale of 1:250 is considered in computational modeling and the geometrical limits are based on the work developed by Huang *et al.* (2007). Therefore, only scaled data, such as geometrical, physical and mechanical properties, is presented in this example.

Figure 1 – Geometrical characteristics and boundary conditions defined for the CAARC building analysis



Source: Authors (2023)

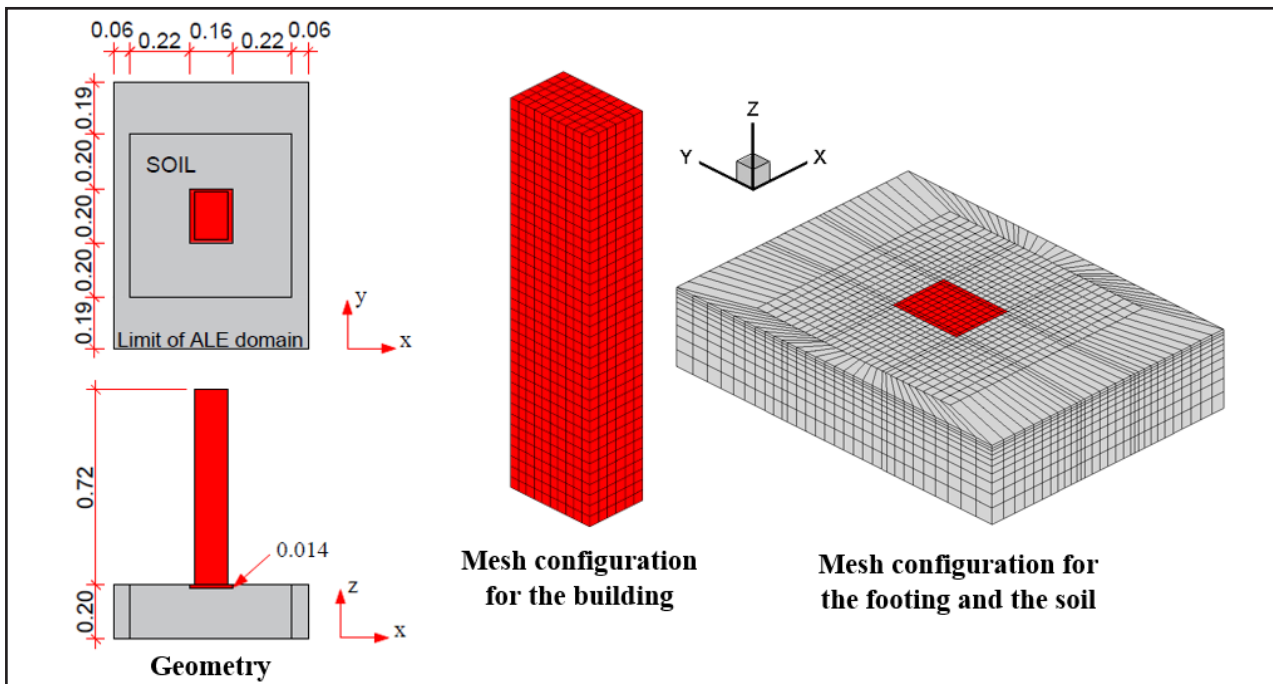
A mesh convergence study was performed and the chosen mesh for the fluid field is composed of 532,715 hexahedral elements and 515,424 nodes, where the minimum element height is about 2×10^{-3} m.

The aeroelastic behavior of the CAARC building model is studied in the present work considering different support conditions and reduced velocities ($V_{red} = V_H/f_n W$, where V_H is the reference velocity at $Z = 0.72$ m, $f_n = 3.161$ Hz is the structural natural frequency and $W = 0.18$ m is the characteristic dimension). A smooth wind flow (with no inflow turbulence) aligned with the X-axis of the computational domain is assumed in the present simulations, which is modeled using a boundary layer profile defined by a power law equation (see Figure 1).

Initially, the building is numerically modeled considering a rigid base (RO model) in order to validate the present algorithm. After that, soil and foundation are added to the numerical models (LEO and NLO models) to evaluate their influence on the aeroelastic response of the structure, whose predictions are compared with the numerical results reported by Shirkhanghah and Kalehsar (2022).

Geometrical characteristics and mesh configurations defined for building structure, foundation and soil modeling are shown in Figure 2. The geometrical limits and mesh configuration defined for the building, footing and soil are based on a mesh independence test and the work developed by Shirkhanghah and Kalehsar (2022). Observe that non-matching meshes between the fluid and deformable solids are utilized. The CAARC building is spatially discretized using 2,220 hexahedral finite elements, considering an arrangement $6 \times 10 \times 37$ according to the global axes. A raft footing is considered in this problem and modeled using 240 hexahedral finite elements with a spatial distribution of $10 \times 12 \times 2$. Building structure and foundation are resting on a soil modeled with 8,760 hexahedral finite elements and 1,200 hexahedral infinite elements, located next to the side walls of the soil computational domain. Initially, the one-point quadrature technique is employed for all elements of the computational mesh. Thus, the model considering a rigid base is spatially discretized using 2,220 hexahedral elements and 2,926 nodes, while the models considering the soil presence are discretized using 11,220 finite and 1,200 infinite hexahedral elements, with a total of 14,971 nodes. Nodes located on the base of the computational domain are totally fixed.

Figure 2 – Geometrical characteristics and mesh configuration defined for the building, footing and soil modeling



Source: Authors (2023)

The footing dimensions are 0.16x0.20x0.014 m, while the soil domain is modeled with the following dimensions: 0.60x0.60x0.20 m. Observe that the geometry of the infinite elements is defined by the geometrical limits of the ALE domain, where mesh motion is permitted. Gravity loads are considered in this problem during the structural analysis, where structural and geostatic initial stress field are defined before wind load application.

The flow Reynolds number $Re = 156,575$ is maintained constant throughout the range of wind velocities analyzed by modifying the dynamic viscosity value, where different time steps are adopted according to the wind reduced velocity, from $\Delta t = 1 \times 10^{-5}$ s to 7.5×10^{-5} s. The specific mass and the volumetric viscosity of the fluid are kept as $\rho = 1.25$ kg/m³ and $\lambda = 0$ Ns/m², respectively, and the artificial parameter c_f is computed for each reduced velocity by setting the Mach number equal to 0.3.

It is assumed that building and foundation structures have elastic behavior. On the other hand, two models are considered for the soil material: one considering

an elastic behavior (LEO model) and the other considering the Drucker-Prager yield criterion (NLO model), assuming coincidence along the outer edges with the Mohr-Coulomb surface. The mechanical properties of the deformable solids are presented in Table 1. Poisson's ratio and Young's modulus are not provided by Shirkhaghah and Kalehsar (2022) for the foundation mechanical properties, therefore typical values for reinforced concrete footing with characteristic compressive strength (f_{ck}) equal to 25 MPa are considered.

The structural equation of motion is solved in time domain using the generalized- α method with spectral radius $r_{\alpha} = 0.8$. The aeroelastic analysis is performed considering 20 subcycles and no structural damping is considered in the models.

Contact interface between soil and foundation is considered with a friction coefficient $\mu_c = 0.84$ and different penalty parameters are used here according to the wind reduced velocity, ranging from 8×10^3 N/m to 2.8×10^4 N/m for the normal penalty parameter (k_N) and 2×10^3 N/m to 1.3×10^4 N/m for the tangential penalty parameter (k_T). The previous values are obtained by trial and error until a divergent process is observed and the last convergent values are considered.

Table 1 – Mechanical properties of deformable solids

Building (Elastic)	Young's modulus – E	1.25 x 10 ⁶ N/m ² for along-wind analysis 5.57 x 10 ⁵ N/m ² for across-wind analysis
	Poisson's ratio – ν	0.25
	Specific mass – ρ	160 kg/m ³
Foundation (Elastic)	Young's modulus – E	1.12 x 10 ⁸ N/m ²
	Poisson's ratio – ν	0.20
	Specific mass – ρ	2,400 kg/m ³
Soil (Elastic/Drucker-Prager)	Young's modulus – E	1.082 x 10 ⁶ N/m ²
	Poisson's ratio – ν	0.30
	Specific mass – ρ	2,160 kg/m ³
	Angle of friction – ϕ	46.22°
	Cohesion – c	7.2 N/m ²

Source: Shirkhaghah and Kalehsar (2022)

The natural frequency of the CAARC building model is typically considered to be identical in along-wind and across-wind directions when studied in wind tunnels (Melbourne, 1980; Thepmongkorn *et al.*, 1999). However, this assumption is physically improbable in reality when a solid prism with uniform material properties and rectangular cross-section is considered, as in the present case. The use of hexahedral finite elements for spatial discretization of the CAARC building model leads to different stiffnesses in each direction and, consequently, unequal natural frequencies. Therefore, the aeroelastic response of the building is separated in the present work into along-wind and across-wind responses, where the Young's modulus of the structure is calibrated according to the principal direction studied in order to obtain the same natural frequency used in the wind tunnel tests (see Table 1). In other words, the frequency employed in the wind tunnel tests ($f_n = 3.161$ Hz) is equal to the first and second natural frequencies, respectively, of the along-wind and across-wind numerical models studied here considering a rigid base.

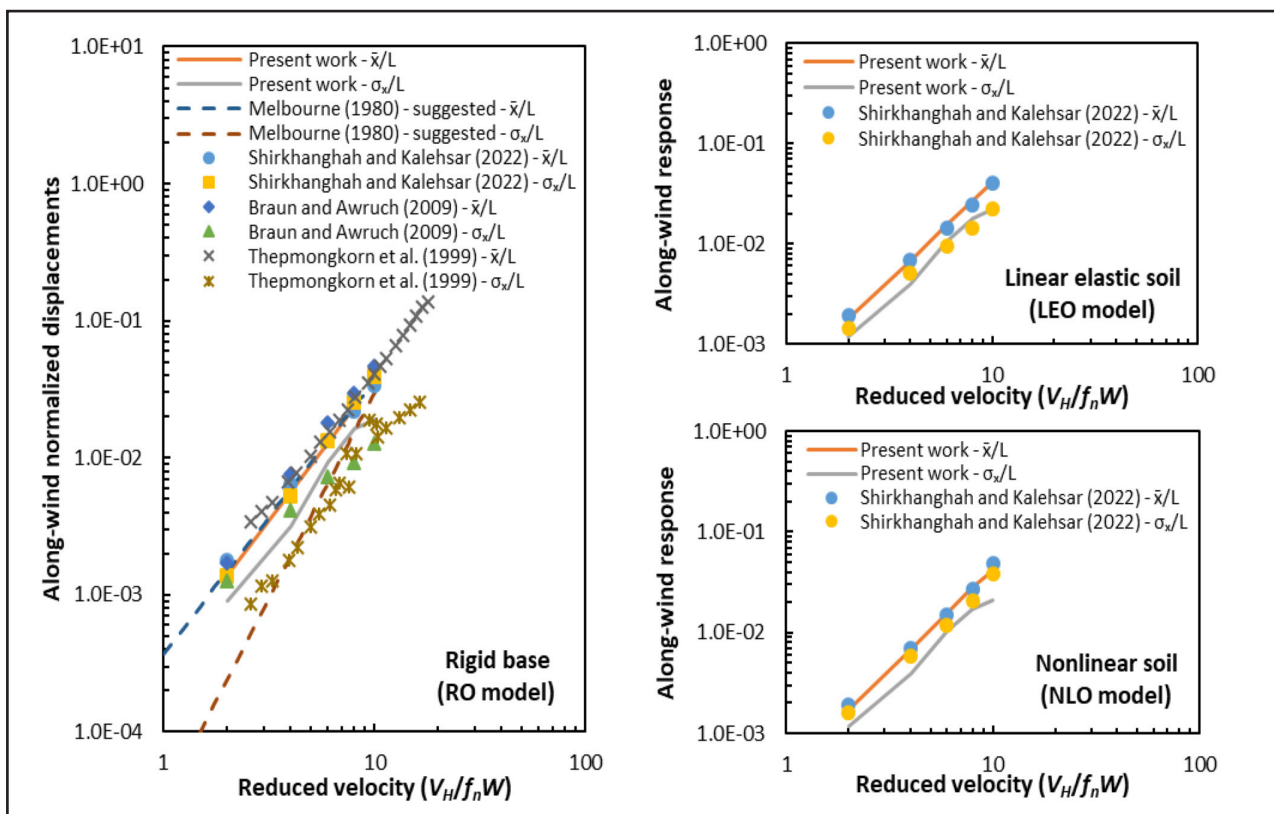
3.1 Along-wind response

The along-wind response of the CAARC building model is studied in this section considering five different reduced velocities: 2, 4, 6, 8 and 10. The flow is initially developed considering the structure as rigid during 3 s, with an initial pressure field equal to zero and initial velocity field equal to the boundary layer profile. The aeroelastic analysis is performed over 2 s after the flow field is fully developed, similar to the numerical analysis developed by Shirkhanghah and Kalehsar (2022).

Mean and standard deviation of longitudinal displacements obtained from the time histories are normalized by the length (L) of the CAARC building and presented in Figure 3 for the different models simulated as functions of the wind reduced velocity. The results obtained here are compared with the suggested curve presented by Melbourne (1980), which represents a best fit to the experimental data, experimental predictions reported by Thepmongkorn *et al.* (1999) and numerical results presented by

Braun and Awruch (2009) and Shirkhaghah and Kalehsar (2022). Notice that the curve obtained here for normalized mean longitudinal displacements (\bar{x}/L), considering the RO model, showed a good agreement with the reference results, particularly with the function proposed by Melbourne (1980). On the other hand, the curve σ_x/L obtained in the present work for RO model is similar to the curves reported by Thepmongkorn *et al.* (1999) and the suggested curve presented by Melbourne (1980).

Figure 3 – Along-wind normalized displacements as functions of the wind reduced velocity



Source: Authors (2023)

Figure 3 shows that the soil presence in the numerical models (LEO and NLO models) led to higher values of \bar{x}/L , on average 20% higher, when compared to the model with rigid base (RO model) for all velocities evaluated in the present work. The same effect was observed with the σ_x/L values. In addition, results obtained in this work for LEO and NLO models are very similar and the curves of \bar{x}/L obtained in this

work for LEO and NLO models showed a good correlation with the results reported by Shirkhanghah and Kalehsar (2022), although some differences can be noted when the curves of σ_x/L are compared. It is important to mention that numerical instabilities were observed during the analysis corresponding to the NLO model, which required the element technology of soil elements to be changed from one-point quadrature to the \bar{B} method in order to ensure numerical stabilization.

A comparison between the average processing time as function of the parallelization technique is presented in Table 2 for the numerical model with rigid base (RO model) and reduced velocity equal to 2. Results presented here can be extended to other reduced velocities without further variations. Numerical simulations are carried out using an AMD Ryzen™ 7 3700X processor, with 16 threads, and a NVIDIA GeForce GTX 1660 Super graphics card, with 1,408 CUDA cores. In addition, numerical simulations are performed using the cluster FERMI provided by the National Center for Supercomputing (CESUP), which operates with an Intel® Xeon® Silver 4116 processor, with 24 threads, and a NVIDIA Tesla P100 graphics card, with 3,584 CUDA cores.

Table 2 shows that the parallelization techniques provided a significant reduction in the processing time when compared to the serial approach. Furthermore, results obtained referring to the CUDA-OpenMP approach using a basic graphics card with single precision variables showed a similar performance to that presented by a professional graphics card dedicated to performing math operations with double precision variables, with no loss of response quality. Despite the higher average processing time observed when the structure is analyzed, it was possible to observe that a significant portion of this time corresponds to compute the mesh velocity field related to the mesh motion of nodes within the moveable region of fluid domain, which is performed by graphics card. Thus, the update of kinematical conditions consists of a step of high computational demand, even for parallel processing with GPUs, and the subcycling algorithm is essential to obtain a more efficient algorithm.

Table 2 – Processing times obtained for RO model and $V_{red} = 2$

Processing approach	Time per step without structure	Time ratio	Time per step with structure	Time ratio
Serial	5.13334 s	100%	20.79233 s	100%
OpenMP	0.53495 s	10.42%	1.68918 s	8.12%
CUDA-OpenMP (DP)	0.24934 s	4.86%	1.47013 s	7.07%
CUDA-OpenMP (SP)*	0.12432 s	2.42%	0.33207 s	1.60%
CESUP - CUDA- OpenMP (DP)	0.11807 s	2.30%	0.41504 s	2.00%

Source: Authorship (2023)

* single precision was used only in the variables related to the fluid analysis.

3.2 Across-wind response

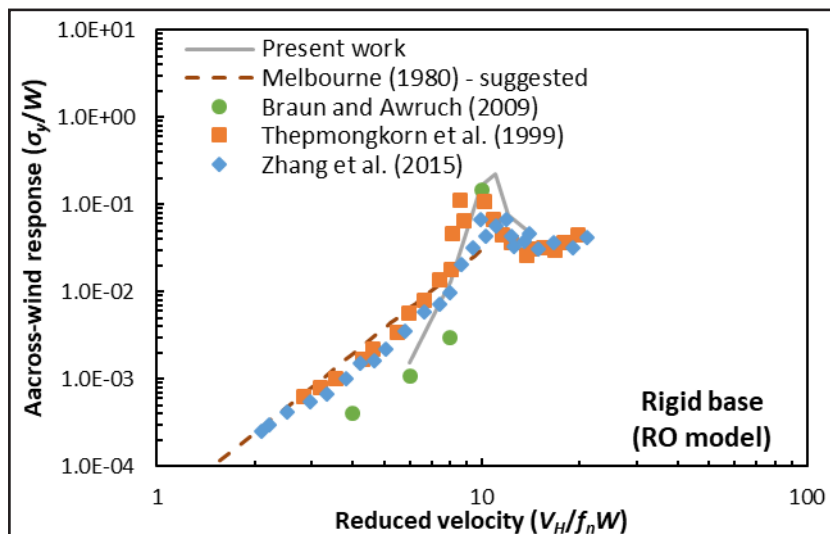
The across-wind response of the CAARC building model is studied in this section in order to investigate the aeroelastic instability induced by vortex shedding phenomenon. This phenomenon is commonly known as *lock-in* and may occur when the vortex shedding frequency of the flow field around the building is near the natural frequency of structure in the transverse direction, leading to greater body movement in the across-wind direction due the strong interaction developed between the structure and the flow.

Considering that the lock-in phenomenon may be induced when a synchronization is observed between the mechanical frequency (f_n) and the vortex shedding frequency (f_v), i.e. $f_n = f_v$, it is possible to obtain a critical speed $V_{cr} = 6.32$ m/s or $V_{cr,red} = V_{cr}/f_n W = 11.1$ (Braun and Awruch, 2009), which represents the wind speed that theoretically induces the lock-in phenomenon. Therefore, six different wind speed levels are chosen to investigate the wind-induced vibration of the CAARC building, corresponding to the following reduced velocities: 6, 8, 10, 11, 12 and 14.

The flow is initially developed considering the structure as rigid during 3 s, with an initial pressure field equal to zero and initial velocity field equal to the boundary layer profile. The aeroelastic analysis is performed over 17 s after the flow field is fully developed, completing 20 s of numerical analysis.

Standard deviation of transversal displacements obtained from the time histories of the RO model is normalized here by the width (W) of the CAARC building and presented in Figure 4. Results obtained in the present work are compared with the suggested curve presented by Melbourne (1980), experimental predictions reported by Thepmongkorn *et al.* (1999) and numerical results presented by Braun and Awruch (2009) and Zhang *et al.* (2015). It is possible to observe that predictions computed here are similar to the reference results, with small differences in the lower range of reduced velocities. In addition, a distinct peak is verified in the present work, close to the theoretical critical speed ($V_{c,red} = 11.1$), which agrees with the peaks reported by Thepmongkorn *et al.* (1999) and Zhang *et al.* (2015).

Figure 4 – Standard deviation of across-wind response as functions of the reduced velocity

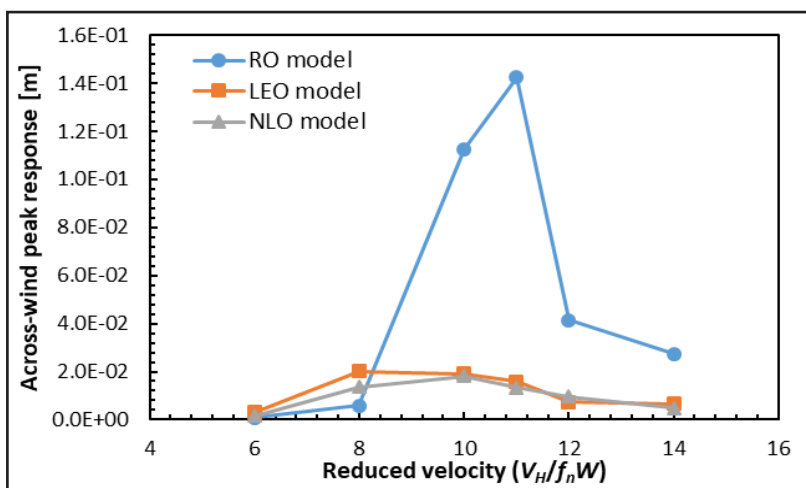


Source: Authors (2023)

Figure 5 presents the across-wind peak response ($|u_y|_{max}$) evaluated at the top of the building for the three numerical models (RO, LEO and NLO models) according to the six reduced velocities studied. One can observe that the aeroelastic instability arises near the critical reduced velocity for the numerical model with rigid base, showing the highest transversal amplitudes. After this region of instability, the synchronization between structural and vortex shedding frequencies is no longer

present and the amplitudes return to a lower level. In contrast, it is clear that the soil-structure interaction affected the structural response and the across-wind peak response is substantially reduced when compared with the results presented by the models with rigid base near the lock-in region, similar to the analytical results reported by Novak and Hifnawy (1988) for chimneys. The numerical model with rigid base showed a transversal displacement peak 8.91 and 10.64 times greater than the results obtained with LEO and NLO models, respectively, when $V_{red} = 11$.

Figure 5 – Across-wind peak displacements as functions of the wind reduced velocity



Source: Authors (2023)

4 CONCLUSIONS

Wind-induced response of the CAARC standard tall building model resting on a deformable soil was numerically evaluated in the present work. The aeroelastic analyses were separated into along-wind and across-wind directions in order to obtain the same natural frequency used in the wind tunnel tests for each direction. Results obtained in the present work for both directions showed a good agreement with the reference results. Regarding the along-wind response, the soil presence led to higher values of mean longitudinal displacements when compared to the model with rigid base. Concerning the across-wind response, numerical results presented a distinct

peak of displacement near the lock-in region for the model with rigid base, which is significantly reduced when the soil-structure interaction is considered. The hybrid CUDA-OpenMP approach showed a significant reduction in the processing time when compared to the corresponding serial algorithm and the processing times showed that it is crucial to use the subcycling algorithm to obtain a more efficient algorithm.

ACKNOWLEDGEMENTS

The authors would like to thank CNPq and CAPES (Brazilian Councils of Research) for the financial support and CESUP/UFRGS (National Center for Supercomputing) for the computational resources.

REFERENCES

- BLOCKEN, B. 50 years of computational wind engineering: past, present and future. **Journal of Wind Engineering and Industrial Aerodynamics**, v. 129, p. 69-102, 2014.
- BRAUN, A. L.; AWRUCH, A. M. Aerodynamic and aeroelastic analyses on the CAARC standard tall building model using numerical simulation. **Computers & Structures**, v. 87, n. 9-10, p. 564-581, 2009.
- HUANG, S.; LI, Q. S.; XU, S. Numerical evaluation of wind effects on a tall steel building by CFD. **Journal of Constructional Steel Research**, v. 63, n. 5, p. 612-627, 2007.
- JIA, J. **Soil Dynamics and Foundation Modeling: Offshore and Earthquake Engineering**. Cham: Springer, 2018.
- LIU, M. Y.; CHIANG, W. L.; HWANG, J. H.; CHU, C. R. Wind-induced vibration of high-rise building with tuned mass damper including soil-structure interaction. **Journal of Wind Engineering and Industrial Aerodynamics**, v. 96, n. 6-7, p. 1092-1102, 2008.
- MADALOZZO, D. M. S.; BRAUN, A. L.; AWRUCH, A. M.; MORSCH, I. B. Numerical simulation of pollutant dispersion in street canyons: geometric and thermal effects. **Applied Mathematical Modelling**, v. 38, p. 5883-5909, 2014.
- MELBOURNE, W. H. Comparison of measurements on the CAARC standard tall building model in simulated model wind flows. **Journal of Wind Engineering and Industrial Aerodynamics**, v. 6, n. 1-2, p. 73-88, 1980.
- MENGLIN, L.; HUAIFENG, W.; XI, C.; YONGMEI, Z. Structure-soil-structure interaction: Literature review. **Soil Dynamics and Earthquake Engineering**, v. 31, n. 12, p. 1724-1731, 2011.

NOVAK, M.; HIFNAWY, L. E. Structural response to wind with soil-structure interaction. **Journal of Wind Engineering and Industrial Aerodynamics**, v. 28, n. 1-3, p. 329-338, 1988.

SHIRKHANGHAH, B.; KALEHSAR, H. E. The Effects of Height and Plan on the Along-Wind Response of Structures Considering Wind-Soil-Structure Interaction. **Journal of Applied Engineering Sciences**, v. 10, n. 2, 2020.

SHIRKHANGHAH, B.; KALEHSAR, H. E. The effect of soil-structure interaction on the along-wind response of high-rise buildings. **Proceedings of the Institution of Civil Engineers-Structures and Buildings**, v. 175, n. 4, p. 332-346, 2022.

THEPMONGKORN, S.; KWOK, K. C. S.; LAKSHMANAN, N. A two-degree-of-freedom base hinged aeroelastic (BHA) model for response predictions. **Journal of Wind Engineering and Industrial Aerodynamics**, v. 83, n. 1-3, p. 171-181, 1999.

THIBAUT, J. C.; SENOCAK, I. Accelerating incompressible flow computations with a Pthreads-CUDA implementation on small-footprint multi-GPU platforms. **The Journal of Supercomputing**, v. 59, n. 2, p. 693-719, 2012.

VENANZI, I.; SALCIARINI, D.; TAMAGNINI, C. The effect of soil-foundation-structure interaction on the wind-induced response of tall buildings. **Engineering Structures**, v. 79, p. 117-130, 2014.

VISINTAINER, M. R. M. **Um modelo numérico para a simulação de problemas de interação fluido-estrutura-solo na Engenharia do Vento**. 2022. 264 p. Tese (Doutorado em Engenharia Civil) – Universidade Federal do Rio Grande do Sul, Porto Alegre, 2022.

ZHANG, Y.; HABASHI, W. G.; KHURRAM, R. A. Predicting wind-induced vibrations of high-rise buildings using unsteady CFD and modal analysis. **Journal of Wind Engineering and Industrial Aerodynamics**, v. 136, p. 165-179, 2015.

Authorship contributions

1 – Michael René Mix Visintainer

PhD in Civil Engineering from the Universidade Federal do Rio Grande do Sul.

<https://orcid.org/0000-0002-0950-3873> • michaelrene@gmail.com

Contribution: Conceptualization, Investigation, Methodology, Software, Validation, Visualization, Writing – original draft, Writing – review and editing.

2 – Alexandre Luis Braun

PhD in Civil Engineering from the Universidade Federal do Rio Grande do Sul.

<https://orcid.org/0000-0002-6170-3653> • alexandre.braun@ufrgs.br

Contribution: Conceptualization, Methodology, Software, Supervision, Writing – original draft, Writing – review and editing.

How to quote this article

VISINTAINER, M. R. M.; BRAUN, A. L. A numerical investigation on the wind-induced response of a high-rise building considering the soil-structure interaction. **Ciência e Natura**, Santa Maria, v. 45, spe. n. 3, e74430, 2023. DOI 10.5902/2179460X74430. Available from: <https://doi.org/10.5902/2179460X74430>. Accessed in: day month abbr. year.